The Journal of Chemical Physics

Fluctuations and asymmetry via local Lyapunov instability in the time-reversible doubly thermostated harmonic oscillator

Cite as: J. Chem. Phys. **115**, 5744 (2001); https://doi.org/10.1063/1.1401158
Submitted: 14 May 2001 . Accepted: 17 July 2001 . Published Online: 17 September 2001

Wm. G. Hoover, H. A. Posch, and Carol G. Hoover

AIP Publishing

Fluctuations and asymmetry via local Lyapunov instability in the time-reversible doubly thermostated harmonic oscillator

Wm. G. Hoover[a)]
Department of Applied Science, University of California at Davis/Livermore and Lawrence Livermore National Laboratory, Livermore, California 94551-7808

H. A. Posch
Institute for Experimental Physics, University of Vienna, Boltzmanngasse 5, A-1090 Vienna, Austria

Carol G. Hoover
Methods Development Group, Lawrence Livermore National Laboratory, Livermore, California 94551-7808

(Received 14 May 2001; accepted 17 July 2001)

Forward and backward trajectories from time-symmetric equations of motion can have time-asymmetric stability properties, and exhibit time-asymmetric fluctuations. *Away* from equilibrium this symmetry breaking is the mechanical equivalent of the second law of thermodynamics. *Strange attractor* states obeying the second law are time-reversed versions of (unobservable) *repeller* states which violate that law. Here, we consider both the equilibrium and the nonequilibrium cases for a simple deterministically thermostated oscillator. *At* equilibrium the extended phase-space distribution is a smooth Gaussian function. *Away* from equilibrium the distribution is instead a fractal strange attractor. In both cases we illustrate local time-symmetry breaking. We also quantify the forward–backward fluctuation asymmetry for the thermostated oscillator. © *2001 American Institute of Physics*. [DOI: 10.1063/1.1401158]

I. INTRODUCTION

Conservative mechanics, whether Newtonian, Lagrangian, or Hamiltonian, is *time-reversible*. To any set of time-ordered coordinates $\{q\}$ satisfying the dynamical equations at times $\{0,dt,2dt,\ldots,t\}$ corresponds a second coordinate set, with the time ordering reversed, which satisfies the *same* motion equations. This time symmetry has been much discussed.[1–6] We illustrate time symmetry here with a *discrete* set of coordinates $\{q\}$, equally spaced in time, to emphasize our interest in understanding the results of time-reversible computer simulations.

A robust treatment of stationary nonequilibrium systems requires thermostat forces.[1,5,6] These extract the heat generated by irreversible processes and are also useful for simulating equilibrium systems. For systems at equilibrium the time direction is not important. Nonequilibrium systems are different. Despite the formal time reversibility of these thermostat forces the *forward* time direction inevitably generates a strange attractor, while the reversed direction generates an unobservable mirror-image repeller. This suggests, correctly, that the time reversibility of the nonequilibrium equations is a bit illusory. We investigate and reinforce this viewpoint here by quantifying the Lyapunov instability of both equilibrium and nonequilibrium systems. Significant stability differences do distinguish the forward and backward time evolutions, and their corresponding fluctuations as well, even in the simplest of nonequilibrium stationary states. Previous investigations which established the lack of symmetry[7–9] are extended here by making a quantitative measure of the asymmetry, based on nonequilibrium fluctuations.

In the present work we review the definition of the "local" instantaneous Lyapunov instability spectrum. This spectrum is the fundamental measure of stability. We stress the importance of time's arrow to the fluctuations in this spectrum, even for a time-reversible dynamics. Though our conclusions are generally valid, we illustrate them for a simple, stationary, nonequilibrium model, the doubly thermostated harmonic oscillator in a temperature gradient.

The equilibrium version of this oscillator was first studied by Martyna, Klein, and Tuckerman.[10] Their interest was to induce canonical-ensemble ergodicity for the oscillator by generalizing Nosé's singly thermostated approach. Holian, Posch, and Hoover[11] then used an elaboration of the model to study several alternative simulation techniques for determining free-energy differences. A different approach to the canonical ensemble was pursued by Hoover and Holian,[12] who controlled not only the kinetic energy, as did Nosé, but also its fluctuation. Subsequently, nonequilibrium versions of this latter thermostat and the earlier one were studied in an effort to characterize the fractal distributions arising far from equilibrium.[13,14] The present work is a continuation of these efforts to understand simple systems out of equilibrium.

We consider relatively long unstable periodic orbits as well as averages over the entire ergodic phase space. We show that the equilibrium behavior of this oscillator on an unstable periodic orbit exhibits part of the complex behavior associated with ergodic nonequilibrium attractors.

a)Electronic mail: hoover3@llnl.gov

II. LYAPUNOV INSTABILITY

Lyapunov instability is the exponential growth, proportional to $e^{\lambda t}$, of the separation between neighboring phase-space trajectories. This instability is the common feature of "chaotic" dynamical systems, both at and away from equilibrium. In equilibrium Hamiltonian mechanics, both the "local" (instantaneous) Lyapunov exponents and their "global" long-time averages occur in "pairs" $\{+\lambda,-\lambda\}$; $\{\langle+\lambda\rangle,\langle-\lambda\rangle\}$. There is a local and a global Lyapunov pair for each coordinate–momentum pair in the Hamiltonian. The pairing symmetry follows directly from Hamilton's equations of motion. It guarantees that Hamilton's equilibrium equations contain no "arrow of time."

Most nonequilibrium systems exhibit Lyapunov instability too.[5,15] It was an unexpected consequence of particular time-reversible forms of nonequilibrium motion equations that a "pairing" reminiscent of equilibrium Hamiltonian mechanics could be established. The circumstances under which pairing occurs away from equilibrium are rather restricted.[16]

III. THERMOSTATED MECHANICS

In the early 1970s Ashurst developed thermostated computer simulations of nonequilibrium steady states.[17] At that time, and even 10 years later, most of the corresponding formal mathematical activity was concerned with promoting ergodicity in equilibrium systems.[18] Nosé introduced a breakthrough in 1984. He used an extended phase space, with an extra friction variable, to simulate Gibbs' equilibrium canonical ensemble.[19] Nosé's thermostated mechanics has turned out to be even more useful *away* from equilibrium than *at* equilibrium.[5]

Typically, deterministic dynamical thermostats are used to control either the instantaneous or the long-time-averaged temperature, $T\equiv\langle p^2/mk\rangle$, where p is a Cartesian momentum component. It is also possible, as shown by Hoover and Holian,[12] and elaborated by Liu and Tuckerman,[20] to control the fluctuations of the kinetic energy by thermostating other moments, such as $\langle p^4\rangle$. Because the positive moments of the kinetic energy all converge, even for simple one-dimensional systems, we choose to focus on the temperature T rather than on the alternative inverse temperature $\beta\equiv 1/kT$. Thermostat forces, such as those used by Ashurst and Nosé, though formally "time reversible," can effectively destroy the forward–backward time symmetry, at least in the case of the local Lyapunov exponents, even at equilibrium, where there is no long-term tendency for phase volume to decrease.

We accept here the physicist's definition of "time reversibility:" motion equations generating a time-ordered coordinate set

$$\{q_0,q_{dt},q_{2dt},\ldots,q_t\},$$

and time-ordered sets of "momentum-like" variables

$$\{p_0,p_{dt},p_{2dt},\ldots,p_t\},$$

are said to be time reversible provided that the sets $\{+q,-p\}$ satisfy *exactly the same motion equations* but with the time order of the sets reversed [so that the reversed motion proceeds from $(q_t,-p_t)$ back to $(q_0,-p_0)$].

IV. NOSÉ–HOOVER OSCILLATOR

The simplest mechanical model including time-reversible deterministic thermostat forces is the Nosé–Hoover oscillator,[21] an oscillator with its mean-squared momentum "controlled" by the friction coefficient ζ. For simplicity we choose the oscillator mass and force constant, as well as the relaxation time governing the friction coefficient, all equal to unity. In this (typical) case, the oscillator is governed by the *time-reversible* motion equations

$$\{\dot q=p;\dot p=-q-\zeta p;\dot\zeta=p^2-1\}.$$

From the stationary long-time average of the $\dot\zeta$ equation we infer that $\langle p^2\rangle_{t\to\infty}\equiv 1$. Note that in the time-reversed motion both the momentum p and the "control variable," the friction coefficient ζ, change sign. The friction coefficient ζ gives directly the instantaneous time rate of change of an infinitesimal element of phase volume $\otimes$, Gibbs' "extension in phase"

$$\dot\otimes/\otimes=(\partial\dot q/\partial q)+(\partial\dot p/\partial p)+(\partial\dot\zeta/\partial\zeta)=-\zeta.$$

Though relatively simple, the Nosé–Hoover oscillator motion is not ergodic. Instead, the (q,p,ζ) oscillator phase space is partitioned into infinitely many Lyapunov-stable ("regular") regions surrounding individual stable periodic orbits. The stable regions are embedded in an unstable chaotic sea which fills the rest of the space.[21]

V. DOUBLY THERMOSTATED HARMONIC OSCILLATOR

In the present work we illustrate the loss of time symmetry with time-reversible motion equations by exploring a slightly more-complicated example, a doubly thermostated harmonic oscillator based on the thermostating ideas of Martyna, Klein, and Tuckerman.[10] For simplicity we again choose all the arbitrary parameters in this model equal to unity. The usual oscillator equations

$$\{\dot q=+p;\dot p=-q\},$$

which generate a constant-energy circle in phase space

$$q^2+p^2=2E,$$

are augmented by adding *two* control variables, ζ and ξ. In the simplest isothermal case, with the temperature everywhere equal to unity, the two controls together generate Gibbs' canonical phase-space distribution

$$f(q,p,\zeta,\xi)\propto e^{-(q^2+p^2+\zeta^2+\xi^2)/2},$$

in the four-dimensional augmented phase space. The augmented equations of motion,

$$\dot q=p;$$

$$\dot p=-q-\zeta p;$$

$$\dot\zeta=p^2-T(q)-\zeta\xi;$$

$$\dot\xi=\zeta^2-T(q);$$

$$T(q)\equiv 1+\epsilon\tanh(q),$$

are *time reversible*. This means that simultaneously reversing the time order of (q,p,ζ,ξ) points along the trajectory while changing the signs of the time and the momentum-like variables (p,ζ,ξ) also gives a solution of the same motion equations.

These motion equations, which focus on controlling fluctuations in the instantaneous kinetic temperature, could alternatively be formulated in terms of $\beta=1/kT$, but we choose not to do so. An approach[12–14] stabilizing not only the kinetic energy, through $\langle p^2\rangle$, but also its fluctuation, through $\langle p^4\rangle$

$$\dot q = p;$$

$$\dot p = -q - \zeta p - \xi p^3;$$

$$\dot\zeta = p^2 - T(q);$$

$$\dot\xi = p^4 - 3p^2 T(q);$$

$$T(q) \equiv 1 + \epsilon \tanh(q),$$

could also be used. At equilibrium a time average of the $\dot\zeta$ equation shows that $\langle p^2\rangle \equiv T$, a desirable property not shared by the Martyna–Klein–Tuckerman equations. But, away from equilibrium the time average guarantees only that the spatially averaged kinetic temperature agrees with the spatially averaged T. Explicit calculations (kindly suggested to us by Brad Holian) show that the time-averaged kinetic temperature has a complicated space dependence, with large oscillations about the specified temperature $T(q)$. For temperature gradients ($\epsilon > 0.2632$) larger than those we treat here the solution of the equations is a stable limit cycle. These stable cycles persist, at least in all those cases which we have investigated, even for ($\epsilon > 1$) and correspond to *negative* temperatures for sufficiently negative coordinate values.

Three simple mathematical considerations suggest that the Martyna–Klein–Tuckerman (MKT) oscillator is a better choice for analysis than is the Hoover–Holian oscillator: first, the quadratic equations have two unstable fixed points[10] to which a mathematical analysis could be tied; second, quadratic forces, as opposed to quartic Hoover–Holian forces, should be simpler to treat; finally, the effective Hamiltonian

$$\mathcal{H}_{\rm MKT} \equiv \tfrac{1}{2}(q^2 + p^2 + \zeta^2 + \xi^2),$$

satisfies an interesting identity[9]

$$\dot{\mathcal{H}}_{\rm MKT} \equiv -(\zeta + \xi) T(q),$$

for the local dissipation at q analogous to the thermodynamic relation, $\dot E = \dot S T$. For these reasons of simplicity, here we have adopted the quadratic motion equations rather than the quartic alternative. Likewise, we have refrained from introducing explicit symbols for the oscillator mass, the force constant, the two relaxation times for the thermostat variables, and a scale length in the temperature variation. We focus our attention on the simplest possible interesting case, choosing all these parameters equal to unity. Our main emphasis is on the time symmetry of the solutions and we believe that the symmetry properties of the oscillator would have no surprising dependence on the additional parameter values.

Away from equilibrium the ground rules for thermostating are not clear, with different types of thermostats giving different stationary states. It is sensible, whenever possible, to maintain the fundamental ideal-gas temperature definition, $\langle p^2/mk\rangle \equiv T$. It is not at all clear how p^4 or p^6 or even p^3 should be constrained away from equilibrium. Simplicity is the only guide. For the hyperbolic-tangent temperature profile isothermal equilibrium, with $T=1$, corresponds to the choice $\epsilon = 0$. In the *nonequilibrium* case there is a *temperature gradient*, with the maximum gradient (at $q=0$) equal to ϵ. The equations of motion are still time reversible. It is easy to see that reversing the time (by setting $+dt$ to $-dt$ in the algorithm solving the equations) results in exactly the *same* motion equations provided that the symmetry operations

$$\{p \to -p; \zeta \to -\zeta; \xi \to -\xi; t \to -t\},$$

are simultaneously applied. Physically this means that not only p but also the control variables ζ and ξ behave like momenta.

Although the long-time-averaged Lyapunov exponents are necessarily independent of the initial condition (because the motion is ergodic), numerical simulations[7–9] have shown that the *local* Lyapunov exponents *at* the phase point $\{q, +p, +\zeta, +\xi\}$ are *not* simply related to those at the corresponding time-reversed phase point $\{q, -p, -\zeta, -\xi\}$. This is a symmetry breaking. In view of the fact that the equations governing the motions of neighboring trajectories are strictly time reversible, the lack of correlation between the forward and backward local Lyapunov exponents may come as a surprise. But, it can be understood. The lack of symmetry is the result of the local Lyapunov exponents' dependence on the *past* and not the *future*. This dependence is sufficiently strong that the spatial variation of the local exponents is typically fractal.[7,8] We describe the local exponents' calculation next.

VI. LOCAL LYAPUNOV EXPONENTS

The local Lyapunov exponents quantify the expansion and contraction rates which contribute to $\Sigma_i \lambda_i = \dot\otimes/\otimes$ at every phase-space point. The directions in which these rates are measured represent the integrated past history in the neighborhood of the trajectory passing through the point. There are several algorithms for the numerical evaluation of the local exponents. Here, we describe an elegant Lagrange-multiplier approach[1,5,15] which is the limiting differential-equation representation of finite-difference algorithms developed earlier by Stoddard, Ford, and Benettin.

The four *local* (instantaneous) Lyapunov exponents

$$\{\lambda_{11}, \lambda_{22}, \lambda_{33}, \lambda_{44}\} \equiv \{\lambda_1, \lambda_2, \lambda_3, \lambda_4\},$$

for the thermostated oscillator can be found by solving the four sets of differential equations for the evolution of four nearby oscillator trajectories separated from the reference trajectory by the infinitesimal offset vectors $\{\delta_1, \delta_2, \delta_3, \delta_4\}$

$$\dot\delta_1 = D\cdot\delta_1 - \lambda_{11}\delta_1;$$

$$\dot\delta_2 = D\cdot\delta_2 - \lambda_{12}\delta_1 - \lambda_{22}\delta_2;$$

$$\dot{\delta}_3 = D\cdot\delta_3 - \lambda_{13}\delta_1 - \lambda_{23}\delta_2 - \lambda_{33}\delta_3 ;$$

$$\dot{\delta}_4 = D\cdot\delta_4 - \lambda_{14}\delta_1 - \lambda_{24}\delta_2 - \lambda_{34}\delta_3 - \lambda_{44}\delta_4 .$$

The "dynamical matrix" D is the first derivative of the equations of motion with respect to the phase-space directions. For the doubly thermostated oscillator with quadratic forces, D is as follows:

$$D = \begin{pmatrix} 0 & 1 & 0 & 0 \\ -1 & -\zeta & -p & 0 \\ -\epsilon\cosh^{-2} q & 2p & -\xi & -\zeta \\ -\epsilon\cosh^{-2} q & 0 & 2\zeta & 0 \end{pmatrix}.$$

The constraining multipliers $\{\lambda\}$ are chosen to maintain the orthonormality of the separation vectors $\{\delta\}$

$$\lambda_{ii} = \delta_i\cdot D\cdot\delta_j ; \lambda_{ij} = \delta_j\cdot D\cdot\delta_i + \delta_i\cdot D\cdot\delta_j .$$

It is easy to verify that simultaneously changing the signs of p, ζ, and ξ, along with the signs of the corresponding components of the $\{\delta\}$ gives a second set of separation vectors satisfying exactly the same equations. Thus, any solution of the equations going "forward" in time corresponds to another solution with the signs of p, ζ, and ξ and the signs of the four Lyapunov exponents changed too. The Lagrange multipliers—identical to the local Lyapunov exponents—satisfy the local sum rule

$$\sum_i \lambda_{ii} \equiv \sum_i \lambda_i \equiv \dot{\otimes}/\otimes .$$

The long-time-averaged values of the exponents, or Lagrange multipliers, are the conventional "global" Lyapunov exponents

$$\{\langle\lambda_{ii}\rangle\} = \langle\lambda_i\rangle .$$

VII. TIME REVERSIBILITY

Backward trajectories—"time reversed" relative to the usual *forward*-in-time trajectories—for time-reversible motion equations can in principle be generated in any of three ways. The usual algorithm generating the forward trajectory, with $dt>0$, can be applied to the final state, but with dt everywhere changed in sign (negative). This sign change destroys the stability advantage of contracting (dissipative) flows, replacing the overall contraction by expansion and instability. This sign-change approach ($dt<0$) is the standard mathematicians' way to generate the *Lyapunov-unstable* repeller states which correspond to a map or to a set of differential equations generating an attractor with ($dt>0$).

In Fig. 1 we show projections of two relatively long trajectories for the nonequilibrium doubly thermostated oscillator described in Sec. V. The upper plot shows the transition from repeller to attractor which invariably results with a positive time step. The lower plot represents an exactly similar transition, but from the attractor to the repeller, induced by using a negative time step. For the doubly thermostated oscillator the solutions with positive and negative dt are mirror images of one another, with the values of $\{p,\zeta,\xi\}$ differing only in sign.

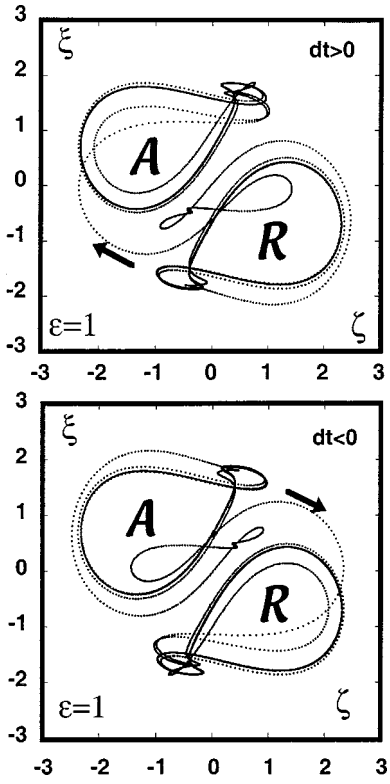

FIG. 1. $(\zeta\xi)$-plane projection of two mirror-image trajectories for the doubly thermostated oscillator with $\epsilon=1$ and a fourth-order Runge–Kutta time step of $dt=\pm 0.002$. The upper plot, with a positive time step, begins on the repeller and ends on the attractor. The lower plot, with a negative time step, begins on the attractor and ends on the repeller. The points generated in the two plots are precise mirror images of each other. The order in which the points are generated is indicated by arrows.

An alternative approach to the generation of a backward trajectory can be based on the *physical* notion of time reversibility—using the same equations but different initial conditions—the final phase-space state(after a time interval t) can first be inverted

$$\{p\to -p, \zeta\to -\zeta, \xi\to -\xi\}.$$

Next, the algorithm can be applied for the same interval with $dt>0$. Finally, a second inversion can be applied to generate the original initial state. Just as in the other approach ($+dt \to -dt$) an initial attractor state is converted to a repeller state by inversion.

Evidently neither of the two approaches just described is capable of precisely recapturing the past. Because the time-reversed motion is even less stable than the original trajectory, the past history is limited by Lyapunov instability. The number of oscillations which can be followed backward in time is of the order of the number of digits carried in the simulation, typically between 10 and 20. In the absence of a quantitative criterion for "near reversibility" we can make no more-precise estimate for corresponding "reversal times."

In the nonequilibrium case the past can only be obtained by storing a trajectory generated in the forward direction. Thus, a third brute-force approach to backward trajectories is actually the *only* effective numerical method: except in very special circumstances, Lyapunov-unstable backward trajecto-

ries can only be constructed from stored forward data. Unstable periodic orbits provide a special circumstance. It should be noted that the time-averaged Lyapunov exponents for strictly periodic orbits *must* obey the symmetry requirement

$$\{+\langle\lambda_{\text{forward}}\rangle\}=\{-\langle\lambda_{\text{backward}}\rangle\}.$$

Surprisingly, other moments can differ. In particular, the second moments of the Lyapunov exponents, forward and backward, turn out to be different in the examples treated here. The second moments for the Martyna—Klein—Tuckerman oscillator are detailed in the tables.

VIII. FLUCTUATIONS

Fluctuations away from equilibrium are of intense interest because they should help to understand the time-symmetry breaking responsible for the formation of multifractal strange attractors in the nonequilibrium phase space. The differences, due to time direction, in local Lyapunov exponents suggest that the fluctuations of these exponents are of particular significance. In the forward direction of time it is easy enough to integrate the time averages $\{\langle\lambda_i^2\rangle\}$. In the present problem these averaged second moments are relatively large, so that there is no important difference between them and the time-averaged fluctuations $\{\langle(\lambda_i-\langle\lambda_i\rangle)^2\rangle\}$. Before proceeding with numerical evaluations of the exponents and their fluctuations, let us consider periodic orbits, which simplify the numerical work by reducing the time required for averaging.

IX. UNSTABLE PERIODIC ORBITS

Poincaré's recurrence theorem establishes that any chaotic ergodic system must necessarily exhibit unstable periodic orbits. We examine such orbits in order to make precise "long-time averages" with a finite amount of computer time. Although such periodic orbits are thought to be commonplace, with the number of them increasing exponentially in their length, it was in fact relatively difficult to find them. We believe that a reason for this difficulty is that the number of such orbits is in fact very restricted. In studying the *numerical* periodic orbits induced by the finite computer wordlength Dellago and Hoover[8] followed up and extended earlier work of Kruskal's, which established that the actual number of periodic orbits is about half the natural logarithm of the number of accessible phase-space states, $\ln\sqrt{\Omega}$. This result, though true, is a bit surprising. Because a randomly generated orbit will intersect itself in a number of steps on order of the square root of the number of states,[8,22] $\sqrt{\Omega}$, one might expect that an exhaustive sampling of all Ω phase-space states would reveal $\sqrt{\Omega}$ different orbits, each with about as many states as the others. In fact, the periodic orbits found by exhaustive enumeration have very different sizes.[8] Typically, the basin of attraction of the largest orbit is huge, on order of Ω rather than of the order of the periodic-orbit length, $\sqrt{\Omega}$. The number of additional periodic orbits is relatively few. Here, we study two different periodic orbits for the Martyna–Klein–Tuckerman oscillator, one at equilibrium and one away from equilibrium. For the numerical work we have adopted the method developed by Diakonos, Schmelcher, and Biham and applied by them to the Hénon map.[23]

We follow Diakonos, Schmelcher, and Biham by considering the unstable Poincaré map $\mathcal{P}$:

$$x_{n+1}=\mathcal{P}(x_n)+\mu C\cdot[\mathcal{P}(x_n)-x_n].$$

Here, C is a matrix, 3×3 in our case, selected from a set of 48 orthogonal matrices with only one element equal to ±1 in each row or column and all other elements vanishing. C equal to the unit matrix turned out to be the most useful choice in our case. The small parameter μ, of order 0.01 to 0.1, selectively stabilizes those periodic orbits with Lyapunov exponents smaller than a critical value. For $\mu=0$ the same orbit is unstable. In our oscillator work we use the $q=0$ plane for constructing the map $\mathcal{P}$.

Despite the relative rarity and special nature of unstable periodic orbits, these orbits do have useful conceptual consequences. At equilibrium, for instance, any unstable periodic orbit with different numbers of positive and negative Lyapunov exponents has an equally likely twin with these numbers reversed. Therefore, despite the asymmetric distribution of Lyapunov exponents on periodic orbits, any fully ergodic phase-space average must lead to equal numbers of positive and negative exponents. Our results for the doubly thermostated oscillator, detailed in the next section, are in accord with this conclusion.

X. NUMERICAL RESULTS

As usual, we use the classic fourth-order Runge–Kutta integrator in our numerical work, choosing the time step dt sufficiently small to avoid influencing our results. Strictly time-reversible algorithms, of the type discussed by Brańka and Wojciechowski[24,25] and by Jang and Voth,[26] cannot be formulated so as to capture the many-to-one contracting dynamics associated with dissipative nonequilibrium states.[1]

A. Exponents for periodic orbits

Figures 2 and 3 show the local Lyapunov exponents λ_1 and λ_4 for short trajectory segments along both equilibrium and nonequilibrium unstable periodic orbits. The curves marked "forward" correspond to the usual solution of the equations of motion. The curves marked "backward" correspond to mirror-image periodic orbits in which the p, ζ, and ξ values are changed in sign and the ordering of the points is reversed. The time-averaged exponents of the forward and backward trajectories have identical magnitudes but differ in sign. The local values show no such simple correspondence. The fluctuations of the local values are given in Table I. To eliminate transients in the orientations of the offset vectors it is necessary to follow the orbits several times. The forward–backward differences are significant, both at and away from equilibrium. We were surprised to find that two of the four offset vectors associated with the local Lyapunov exponents changed sign in the course of a periodic orbit. This corresponds to a systematic rotation in phase space in the neighborhood of the periodic orbit. Thus, the time period required for all four δ vectors to regain their original orientations is *twice* the periodic-orbit time.

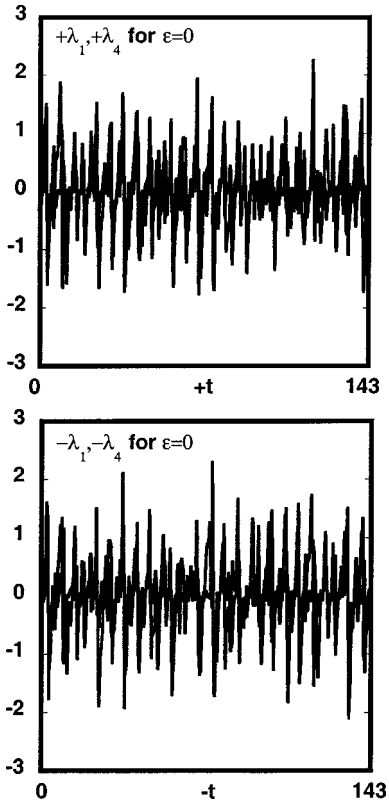

FIG. 2. Local Lyapunov exponents, both forward and backward in time, on an unstable periodic orbit for an *equilibrium* thermostated harmonic oscillator. There is no simple relationship between the two spectra other than the time average, $\langle +\lambda_{i,\mathrm{forward}}\rangle = \langle -\lambda_{5-i,\mathrm{backward}}\rangle$. The initial values of q,p,ζ, and ξ are, respectively, 0.000 000 000 0, +1.204 114 940, +0.055 232 430, and +0.202 910 916. The period is 142.699 121. The time-averaged Lyapunov exponents, and their fluctuations, appear in Table I.

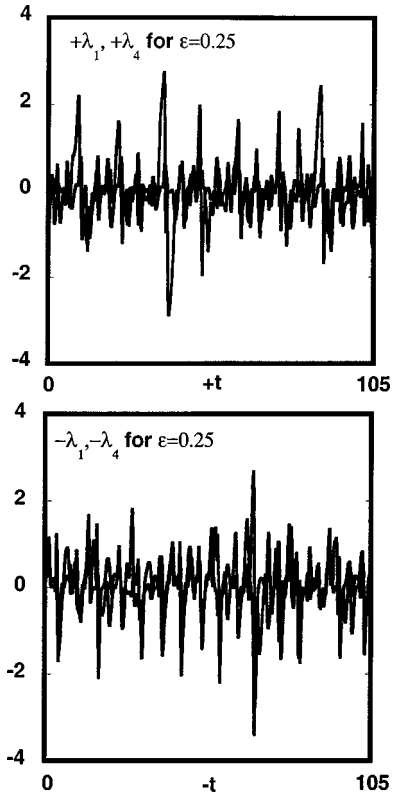

FIG. 3. Local Lyapunov exponents, both forward and backward in time, on an unstable periodic orbit for a *nonequilibrium* thermostated harmonic oscillator. There is no simple relationship between the two spectra other than the time average, $\langle +\lambda_{i,\mathrm{forward}}\rangle = \langle -\lambda_{5-i,\mathrm{backward}}\rangle$. The initial values of q,p,ζ, and ξ are, respectively, 0.000 000 0000, +0.607 855 283 3, +0.492 479 609, and +0.876 059 268. The maximum temperature gradient ϵ is 0.25. The period is 104.885 807. The time-averaged Lyapunov exponents, and their fluctuations, appear in Table I.

B. Exponents for ergodic trajectories

Exponents for fully ergodic flows, at and away from equilibrium, were generated using the Lagrange-multiplier technique described in Sec. VI. As discussed in Sec. VII, the reversed flow could only be generated by storing these trajectories, with the momentum-like variables changed in sign, and processing the data in the reversed direction. *At equilibrium* there are no significant differences. This follows from the fact that the measures of any forward–backward pair of periodic orbits (which can approximate ergodic orbits arbitrarily well) are equal. *Away from equilibrium* the measure of a long backward orbit is negligibly small so that such an orbit is not observable. The data of Table II show that not only the magnitudes of the Lyapunov exponents, but also their fluctuations, differ away from equilibrium. Thus, the fluctuations in the local Lyapunov exponents provide a useful tool for distinguishing nonequilibrium strange attractors.

XI. CONCLUSIONS

Although the equilibrium thermostated equations of motion are time reversible, the forward and backward distributions of the local Lyapunov exponents are distinct. This difference, familiar in the attractors and repellers characterizing nonequilibrium systems, is due to the asymmetry of memory, with the local Lyapunov exponents reminiscent of the past, but not the future. Symmetry breaking can be quantified through the dependence of spectral fluctuations on time's arrow.

The most dramatic way to visualize the time asymmetry is to compare parametric plots (with time as the parameter)

TABLE I. Time-averaged Lyapunov exponents, and their squares, for the unstable periodic orbits of a doubly thermostated harmonic oscillator at thermal equilibrium ($\epsilon=0.00$) and away from equilibrium ($\epsilon=0.25$). For the initial conditions see the figure captions. The initial conditions for the "forward" and "backward" orbits differ only in the signs of p, ζ, and ξ. The exponents sum to zero in both these equilibrium cases, $\epsilon=0.00$. In the corresponding *nonequilibrium* cases the exponent sum forward in time is negative, like that of a strange attractor, while the exponent sum of the orbit's symmetric twin has a positive exponent sum.

ϵ	$\langle\lambda_1\rangle$	$\langle\lambda_2\rangle$	$\langle\lambda_3\rangle$	$\langle\lambda_4\rangle$
0.00f	+0.0188	+0.0000	−0.0040	−0.0148
0.00b	+0.0148	+0.0040	−0.0000	−0.0188
0.25f	+0.0526	+0.0000	−0.0297	−0.1062
0.25b	+0.1062	+0.0297	−0.0000	−0.0526
ϵ	$\langle\lambda_1^2\rangle$	$\langle\lambda_2^2\rangle$	$\langle\lambda_3^2\rangle$	$\langle\lambda_4^2\rangle$
0.00f	+0.425	+0.321	+0.275	+0.194
0.00b	+0.458	+0.316	+0.279	+0.191
0.25f	+0.448	+0.366	+0.231	+0.289
0.25b	+0.388	+0.418	+0.246	+0.388

TABLE II. Long-time-averaged Lyapunov exponents, and their squares, for an ergodic doubly thermostated harmonic oscillator. The exponents sum to zero in the equilibrium case, $\epsilon = 0.00$. In the nonequilibrium case the exponent sum corresponds to the rate of entropy loss to the thermostat, $\dot{S}/k$.

ϵ	$\langle\lambda_1\rangle$	$\langle\lambda_2\rangle$	$\langle\lambda_3\rangle$	$\langle\lambda_4\rangle$
0.00f	+0.069	+0.000	−0.000	−0.066
0.00b	+0.066	+0.004	−0.000	−0.069
0.25f	+0.052	+0.000	−0.033	−0.086
0.25b	+0.086	+0.033	−0.000	−0.052
ϵ	$\langle\lambda_1^2\rangle$	$\langle\lambda_2^2\rangle$	$\langle\lambda_3^2\rangle$	$\langle\lambda_4^2\rangle$
0.00f	+0.452	+0.344	+0.264	+0.283
0.00b	+0.450	+0.341	+0.256	+0.290
0.25f	+0.421	+0.309	+0.222	+0.252
0.25b	+0.350	+0.309	+0.232	+0.329

of the local Lyapunov exponents, forward and backward in time. In Fig. 4 we plot the smallest local Lyapunov exponent as a function of the largest one, both forward and backward in time, for the equilibrium and nonequilibrium periodic orbits detailed in Figs. 2 and 3. Although reversing the time direction for these periodic orbits simply reverses the signs of the two time-averaged exponents, it is apparent that the local values are entirely uncorrelated. Even in the equilibrium case, an unstable periodic orbit of only 10^5 time steps clearly exhibits this breaking of time symmetry. The properties represented here, for a simple microscopic model, are certainly characteristic of macroscopic systems too. This work suggests both a search for a macroscopic variational principle based on nonequilibrium fluctuations, and a careful mathematical analysis of the microscopic dynamics of the doubly thermostated Martyna–Klein–Tuckerman oscillator.

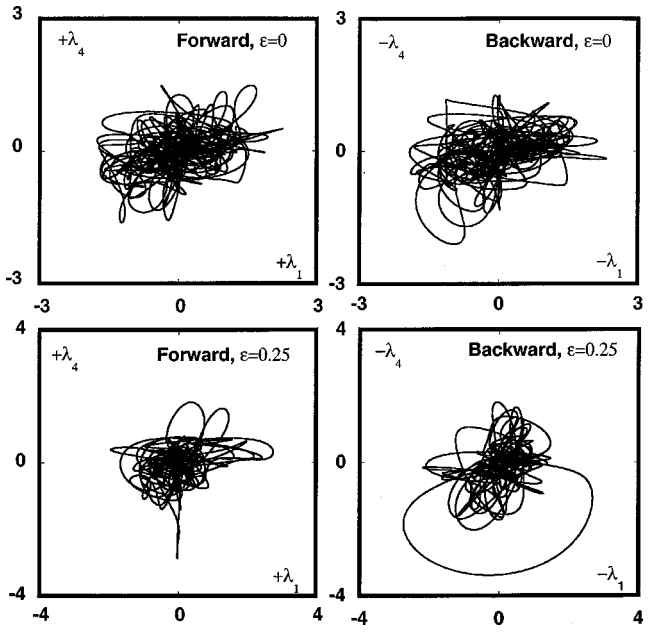

FIG. 4. Parametric dependence of the local Lyapunov exponent λ_4 on λ_1 for both the forward and the backward versions of the periodic orbits described in Figs. 2 and 3. Note that there is no apparent correlation bewtween the exponents in the two time directions.

ACKNOWLEDGMENTS

The work reported here was stimulated by Giovanni Gallavotti. Christoph Dellago read an earlier version of the manuscript. His suggestions are adopted here with thanks. Work in the Methods Development Group at the Lawrence Livermore National Laboratory was performed under the auspices of the United States Department of Energy through University of California Contract No. W-7405-Eng-48. This work was additionally supported by a grant to HAP from the Fonds zur Förderung der Wissenschaftlichen Forschung, Grant No. P11428-PHY.

[1] Wm. G. Hoover, *Time Reversibility, Computer Simulation, and Chaos* (World Scientific, Singapore, 1999).
[2] G. Gallavotti, *Statistical Mechanics* (Springer, Berlin, 1999), Chap. 9.
[3] J. A. G. Roberts and G. R. W. Quispel, Phys. Rep. **216**, 63 (1992).
[4] R. Illner and H. Neunzert, Transp. Theory Stat. Phys. **16**, 89 (1987).
[5] W. G. Hoover, *Computational Statistical Mechanics* (Elsevier, New York, 1991).
[6] D. Ruelle, J. Stat. Phys. **95**, 393 (1999).
[7] Wm. G. Hoover, C. G. Hoover, and D. J. Isbister, Phys. Rev. E **63**, 026209 (2001).
[8] Ch. Dellago and Wm. G. Hoover, Phys. Rev. E **62**, 6275 (2000).
[9] Wm. G. Hoover, C. G. Hoover, and H. A. Posch, Comput Meth. Sci. Tech. **7**, 55 (2001).
[10] G. J. Martyna, M. L. Klein, and M. Tuckerman, J. Chem. Phys. **97**, 2635 (1992).
[11] B. L. Holian, H. A. Posch, and W. G. Hoover, Phys. Rev. E **47**, 3852 (1993).
[12] W. G. Hoover and B. L. Holian, Phys. Lett. A **211**, 253 (1996).
[13] H. A. Posch and W. G. Hoover, Phys. Rev. E **55**, 6803 (1997).
[14] W. G. Hoover and O. Kum, Phys. Rev. E **56**, 5517 (1997).
[15] H. A. Posch and W. G. Hoover, Phys. Rev. A **38**, 473 (1988).
[16] C. P. Dettmann and G. P. Morriss, Phys. Rev. E **53**, R5541 (1996).
[17] W. T. Ashurst, Ph.D. dissertation, University of California at Davis/Livermore (1974).
[18] S. Smale, Proc. N. Y. Acad. Sci. **357**, 260 (1980).
[19] S. Nosé, J. Chem. Phys. **81**, 511 (1984).
[20] Y. Liu and M. E. Tuckerman, J. Chem. Phys. **112**, 1685 (2000).
[21] H. A. Posch, W. G. Hoover, and F. J. Vesely, Phys. Rev. A **33**, 4253 (1986).
[22] C. Grebogi, E. Ott, and J. A. Yorke, Phys. Rev. A **38**, 3688 (1988).
[23] F. K. Diakonos, P. Schmelcher, and O. Biham, Phys. Rev. Lett. **81**, 4349 (1998).
[24] A. C. Brańka, Phys. Rev. E **61**, 4769 (2000).
[25] A. C. Brańka and K. W. Wojciechowski, Phys. Rev. E **62**, 3281 (2000).
[26] S. Jang and G. A. Voth, J. Chem. Phys. **107**, 9514 (1997).